Performance of CI Engines Fuelled with Biodiesel Blends during Transient Operations

B. Tesfa[1a], J Zhu[b] ,F.Gu[a], R. Mishra[a] and A.D.Ball[a]

[a] Center for Efficiency and Performance Engineering, University of Huddersfield, Huddersfield, HD1 3DH, UK

[b] College of Mechanical Engineering, Taiyuan University of Technology, Taiyuan, 030024

In this study the performance characteristics of a CI engine which is fuelled with biodiesel blends during transient conditions were investigated experimentally based on a four-cylinder, four-stroke, direct injection (DI) and turbocharged diesel engine. Different blends from biodiesel and standard diesel (0B, 20B and 100B, 20B means 20% biodiesel and 80% diesel) were tested in the engine operating under two typical transient conditions: the speed varying event and the load varying event. During the experiment, in-cylinder pressure, fuel flow rate and exhaust temperature were measured and detail analyses were carried out on the measured parameters. The analysis conducted on the fuel flow rate shows that the fuel consumption of the engine running with 100B is higher than that of diesel by 16% and 14% for the acceleration and deceleration transient operations respectively. These values increased to 17% and 15% for positive and negative load changes operations. In acceleration and deceleration conditions, the exhaust temperature of engine running with diesel is 2% lower than that of using biodiesel blends. During load transients, the engine running with neat biodiesel produces 7% higher exhaust gas temperature than that of running with diesel. The performance values of 20B blends is in between that of the diesel and neat biodiesel for all key parameters.

Key words: Transient operation, Biodiesel blends, Fuel flow rate, In-cylinder pressure, Exhaust temperature

1- Introduction

A number of extensive investigations have been reported on the engine performance and the emissions of the engine running with biodiesel during steady state operations[1–3]. However, in passenger cars, both steady and transient conditions occur frequently. Transient, in engines, is the change of engine speed and/or torque as a function of time. The transient phenomena can be observed in most automotive drive routes, such as engine start, warm up, accelerations and decelerations due to different road conditions and traffic flows as well as driver' behaviour. Although transient operation has enormous variations regarding to speed and load, it can be represented by two generic transient profiles for the acceleration of Fig. 1(a) and the deceleration of Fig. 1(b). Furthermore, each profile consists of three stages, which are pre-transient steady state condition, transient condition and post-transient condition.

[1] Corresponding author: B.Tesfa, email: b.c.tesfa@hud.ac.uk , Tel: +44 (0) 1484 473532

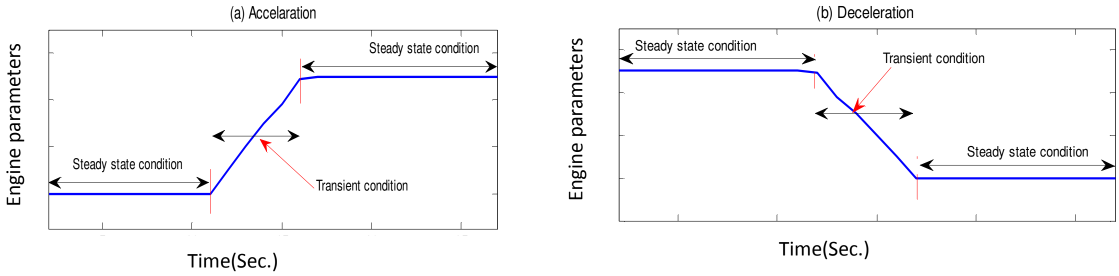

Fig. 1 Speed and Torque transient profile a) acceleration, b) deceleration

The transient phenomena can be initiated by driver's driving behaviour and the slopes and geometric features of the road [4]. It has been reported that road's geometric features, such as road gradients and horizontal road curvatures (roundabouts), considerably influence the performance and emission characteristics of engines [5]. Bazari [5] reported that during the transient process, the performance and emissions characteristics of turbo-charged diesel engines are significantly worse than those under steady conditions. This is mainly because of the difficulties associated with optimising the transient response of the intake, injection and combustion systems. Armas [4] et al. also investigated the effects of biodiesel blends on the smoke-opacity reduction during transient conditions. They reported that the use of biodiesel blends in diesel engines reduces the smoke-opacity significantly, not only in steady conditions, but also during transient engine operations.

In this study, to understand the effects of biodiesel blends on the CI engine performance during transient operations, the fuel consumption rate, exhaust temperature and in-cylinder pressure have been investigated. Since the fuel consumption rate data is more sensitive than the BSFC, the former has been selected to analyse the effects of biodiesel blends on engine performance.

The in-cylinder pressure measurement is considered to be a very valuable source of information during the development and calibration stages of the engine. The in-cylinder pressure signal can provide vital information such as peak pressure, P-V diagram, indicated mean effective pressure, fuel supply effective pressure, heat release rate, combustion duration, ignition delay and so on [6], [7]. Moreover, based on ideal gas and first law of thermodynamics it can be used in more complex calculations for example in air mass flow estimation, combustion diagnosis and NOx prediction [6], [8].

Exhaust gas temperature represents the temperature of the fuel mixture after combustion in the engine cylinder. It can be measured at exhaust manifold. Due to its high sensitivity for dynamic phenomena and its accessibility for measurement, the exhaust gas temperature has been used in detection of combustion anomalies [9], [10], in the design of exhaust gas recirculation (EGR)[11–13] prediction of emission models [14]. Due to this, the exhaust temperature has been selected as parameter to investigate the performance the engine running with biodiesel during a transient condition. Furthermore to get more in-depth information about combustion process in-cylinder pressure values have also been monitored.

Therefore, the objective of this study is to characterise the performance of CI engines based on the fuel flow rate, peak cylinder pressure and exhaust temperature. In section two the experimental facilities and test procedures have been presented. The experimental data from different tests have been analysed with keying findings highlighted correspondingly in section three.

2- Experimental Facilities and Test Procedures

In this study the combustion characteristics and performance of a CI engine running with biodiesel was investigated using a four-cylinder, four-stroke, turbo-charged, water-cooled and direct-injection CI engine. The specifications of the engine are described in Table 1. The transient engine was loaded by a 200kW AC Dynamometer 4-Quadrant regenerative drive with motoring and absorbing capability for both steady and transient conditions.

Table 1 Characteristics of engine [15]

Technical parameters	**Technical data**
Engine type	Turbo charged diesel engine
Number of cylinders	4
Bore	103mm
Stroke	132mm
Compression ratio	18.3:1
Number of valves	16
Injection system	Direct injection
Displacement	4.399 litre
Cooling system	Water
Nominal Idling speed	800 rpm
Maximum rating gross intermittent	74.2 @ 2200rpm
Maximum torque	425Nm @ 1300rpm

The engine test bed was instrumented with speed sensors, pressure transducers, thermocouples, fuel flow metres and in-line torque meter. A Hengler RS58 speed sensor was used to measure the speed of the engine. Fuel flow was measured by a FMS-1000 gravimetric fuel measuring system which was controlled and monitored by CADETV12 software. The cylinder pressure was measured using a Kistler 6125A11 piezo-quartz pressure sensor which was mounted in cylinder 1. The exhaust temperature has been measured by K-type thermocouple with stainless steel wire. The crankshaft position was obtained using a crank angle sensor to determine the cylinder pressure as a function of the crank angle. All the signals collected from the test rig needed to be converted from an original analogue form into a digital form. This was achieved by using a CED Power 1401 Analogue to Digital Converter (ADC) interface between the transducers and a host computer. The CED 1401 power is able to record waveform data, digital (event) data and marker information. It can also generate waveform and digital output simultaneously for real-time, multi-tasking experimental system using its own processor, clocks and memory, under the control of the host computer.

The fuel from biodiesel tank was pumped to a fuel meter and, then it passes through a fuel pump to fuel injectors. The normal diesel was pumped from the main reservoir. The layout of the experimental facilities is described in Fig. 2.

During the testing process the engine was run for 10 minutes to enable it to come to steady state before any measurements were carried out. The frequency of the data acquisition system was at 37 kHz. The maximum rated speed and maximum torque of the test engine is 2200rpm and 425Nm respectively.

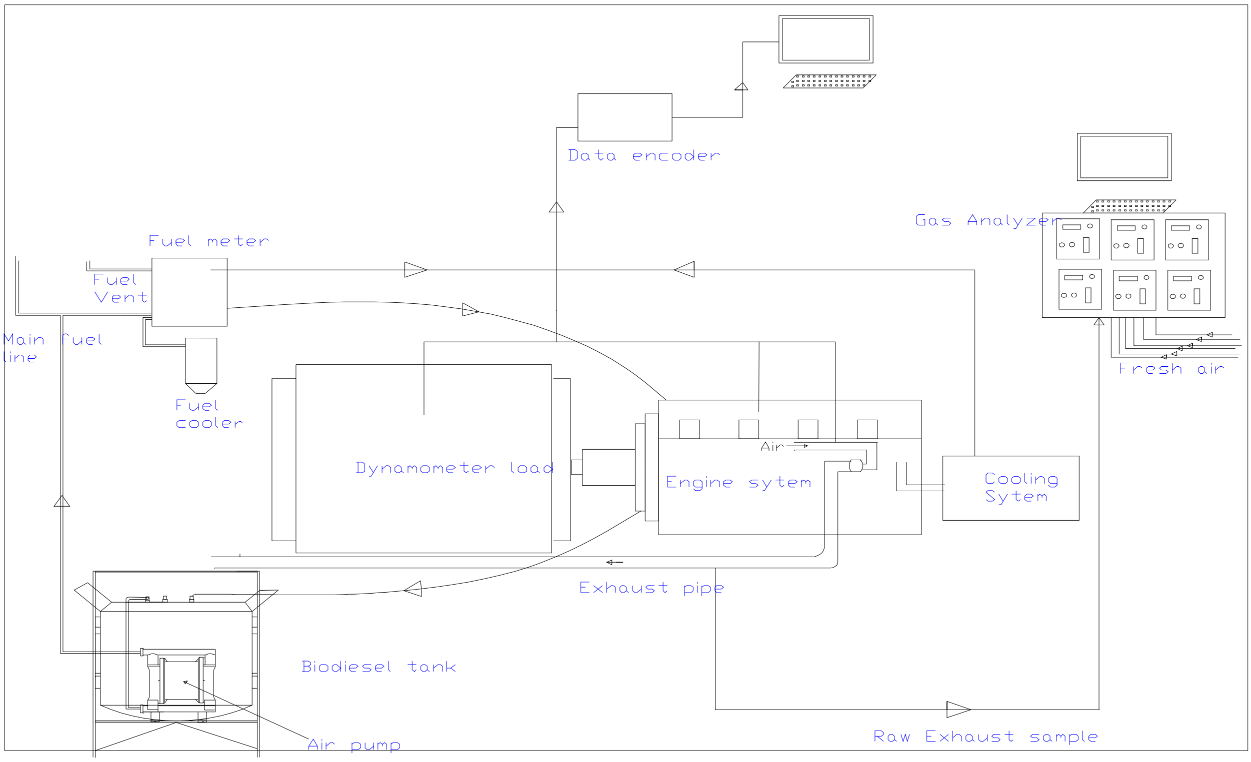

Fig. 2 Engine test facilities lay out [16]

In this study, commercially available biodiesels rapeseed oil biodiesel (ROB obtained from a local company, were used for analysis. The rapeseed oil biodiesel was produced by the transesterfication process from ‘virgin’ oil using methanol. Normal diesel fuel was obtained from a local fuel supplier. The red diesel, which is exactly the same as regular diesel by its combustion, performance and emission behaviour, was used in all tests. The red diesel was selected due to its low fuel tax for off-road engines. The ROB was blended with diesel with the biodiesel percentage volumetric fraction of 0%, 20%, 100%, were formed the blends 0B, 20B, and 100B respectively. The biodiesel and diesel were mixed using the in-tank blending method [5].

For the purpose of this, synthetic speed and torque test cycles were developed in order to study the effect of transients on CI engine performance. The transients were studied during both acceleration and deceleration events independently for both speed and torque transient, as shown in Fig. 3 and Fig. 4.

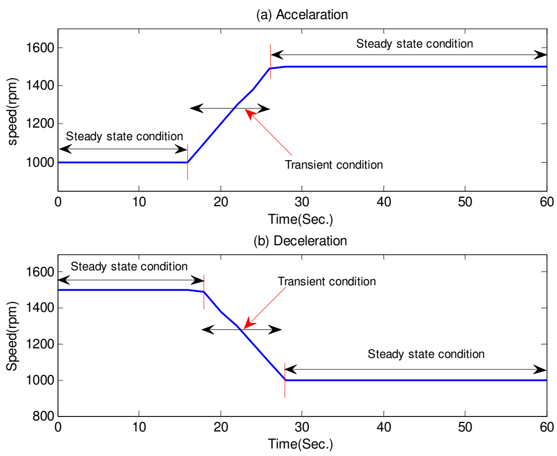

Fig. 3 Speed transient profiles a) Acceleration 1000-1500rpm b) Deceleration (1500-1000rpm)

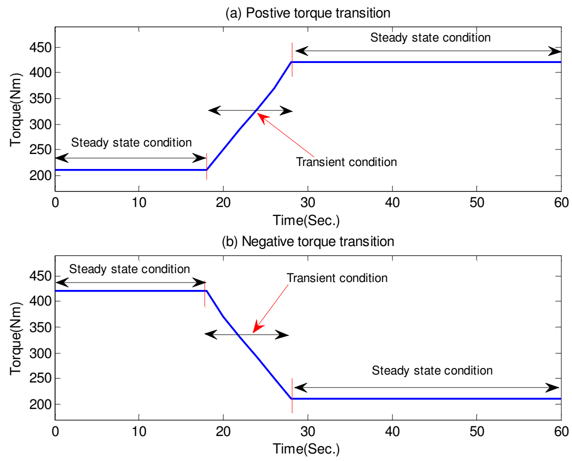

Fig. 4 Torque transition profiles a) Positive torque transition 210-420N b) Negative torque

Fig. 3(a) shows the engine speed acceleration profile for a load value of 420 Nm. Before data collection, the engine was allowed to run for 10 minute to stabilize the operating conditions. During the transient engine test, the acceleration duration normally reported is in the range of 1.0 to 10 seconds [17]. The steady and transient duration used in this test is 17 seconds and 8 seconds respectively, which are within the range specified. Finally, it was run at 1500 rpm for 35 seconds at steady conditions. The deceleration of the CI engine operation is shown in Fig. 3(b). The engine was run steadily for 17 seconds, then decelerated for 8 seconds and then run for 35 seconds at steady conditions. The post-transient steady operation of the engine used was longer than the pre-transient steady operation. This was done in order to study the effects of transient operations on the next steady operation.

The positive and negative torque transition profiles at 1500rpm engine speed are shown in Fig. 4. In this condition, the engine was run for 17 seconds under steady state conditions, then it was run for 8 seconds in transition mode during which torque changed from 210Nm to 420Nm and finally engine was run at 420 Nm for 35 seconds, as presented in Fig. 4(a). Similarly, the engine negative torque transition is shown in Fig. 4(b). In the negative case apart from the torque value, the time segment values are similar to the positive torque transition condition. The rate change of the parameters during transient operation has been calculated by equation (1). This equation is derived from the definition of transient phenomena, which state as transient is change of specified parameter in the given span of time.

$$\dot{Y} = (Y_i - Y_{i-1})/(t_i - t_{i-1}) \quad (1)$$

Where $\dot{Y}$ the rate change of species Y, Y_i is the measured value of parameter at time t_i, $Y_{(i-1)}$ is the measured value of parameter at time t_{i-1}, t_i is latest time step, and t_{i-1} is the previous time-step.

The main physical properties such as composition, density, lower heating value (LHV) and viscosity of the rapeseed oil biodiesel were measured according to the official test standards in EU and published by authors [18]. The blends properties are presented in Table 2.

Table 2 Physical and chemical properties of rapeseed biodiesel and its blends [18].

Property		Diesel(0B)	20B	100B
	C	87	85	77
Composition (%)	H	13	12.8	12
	O	0	2.2	11
Density(kg/m^3)		853.36	865.00	879.30
LHV (MJ/Kg)		42.67	41.84	38.50
Viscosity (mm^2/s)		3.55	4.28	5.13

3- Result and Discussion

3.1- In-cylinder Pressure

One of the most valuable sources of combustion information during the development and calibration stages of the engine is obtained from the in-cylinder pressure. The in-cylinder pressure signal can provide vital information such as peak pressure, P-V diagram, indicated mean effective pressure, injector pressure, heat release rate, combustion duration, ignition delay and so on [6], [7]. In this section the in-cylinder pressure and its dependence on the fuel type have been discussed in detail. The peak in-cylinder pressure corresponding to the speed transient conditions i.e. the speed acceleration from 1000-1500rpm and the speed deceleration from 1500-100rpm are shown in **Error! Reference source not found.**.

As it can be seen in **Error! Reference source not found.**(a), the CI engine fuelled with 100B and 20B resulted in a higher peak in cylinder pressure than the diesel by 15% and 7%, respectively in the transient sections of the operation. This phenomenon is due to the complete combustion of the carbon molecules to yield the maximum torque. The main cause for the higher peak in-cylinder pressure of CI engine running with biodiesel is the advanced combustion process initiated by easy flow-ability of biodiesel derived from the physical properties of biodiesel. In addition, due to the presence of oxygen molecules in biodiesel, the hydrocarbon receives complete combustion. The in-cylinder pressure changes almost uniformly with respect to time in the pre-transient steady operation, as shown in **Error! Reference source not found.**(b). However, due to the effect of the transient operation, during the post-transient operation in-cylinder pressure rate shows some irregularities. During the transient section, the in-cylinder peak pressure attained its peak rate in the middle of the time span of the transient operation.

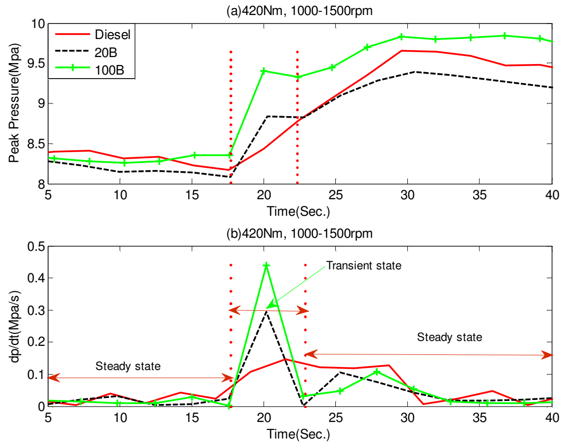

Fig. 5 (a) Variation of in-cylinder peak pressure with time for acceleration (b) in-cylinder peak pressure change rate for acceleration

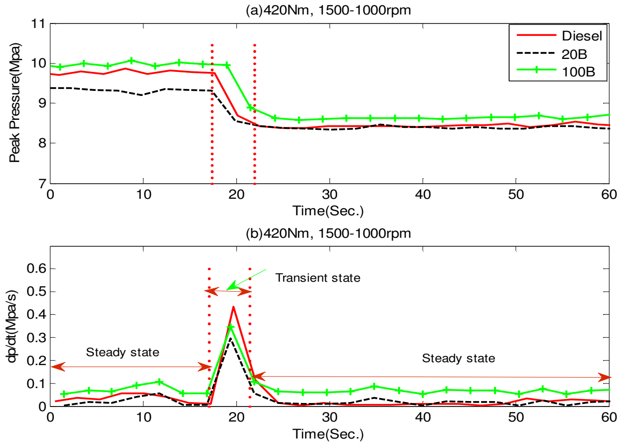

Figure 6 (a) Variation of in-cylinder peak pressure with time for deceleration (b) in-cylinder peak pressure change rate for deceleration

Error! Reference source not found. (a) shows the in-cylinder peak pressure within the CI engine fuelled by diesel, 20B and 100B at a load of 420Nm and a deceleration transient of 1500-1000rpm. Similar to the acceleration transient condition, the CI engine fuelled with 100B resulted in a higher peak in cylinder pressure than the diesel by 5% during the transient section of the operation. The in-cylinder pressure rate changed almost uniformly during pre-transient and post-transient steady state operations, as shown in **Error! Reference source not found.**(b). In the transient section, the engine running with biodiesel blends showed higher in-cylinder peak pressure rates than diesel.

The effects of positive torque transition from 210Nm to 420Nm on the in-cylinder peak pressure when fuelled with diesel, 20B and 100B fuels at 1500rpm, is shown in Fig. 7(a). In the pre-transient section, the diesel followed by 100B, resulted in a higher peak in-cylinder pressure (higher by 9%). However, in the post-transient operation, the engine fuelled by 100B and 20B showed higher in-cylinder pressures than the engine fuelled by diesel by 12% and 6%, respectively. Comparing the in-cylinder pressure rates during the transient section, the 100B resulted in a higher rate than the diesel by 45%, as shown in Fig. 7(b).

Fig. 8 shows the in-cylinder peak pressure when fuelled by diesel, 20B and 100B fuels at a speed of 1500rpm, and during a deceleration torque transient of 420-210Nm. Similar to the acceleration torque transient, the CI engine fuelled with 100B resulted in a higher peak in cylinder pressure than the diesel by 8% in the pre-transient steady section of the operation. However, in post-transient operation, the engine fuelled by the diesel had higher in-cylinder pressure than the engine fuelled by 100B. In the transient section, both 20B and 100B resulted in higher in-cylinder peak pressures. The in-cylinder pressure rate changed irregularly in the three sections. In the transient section, the rate change of the peak in-cylinder pressure was lower than that of the diesel.

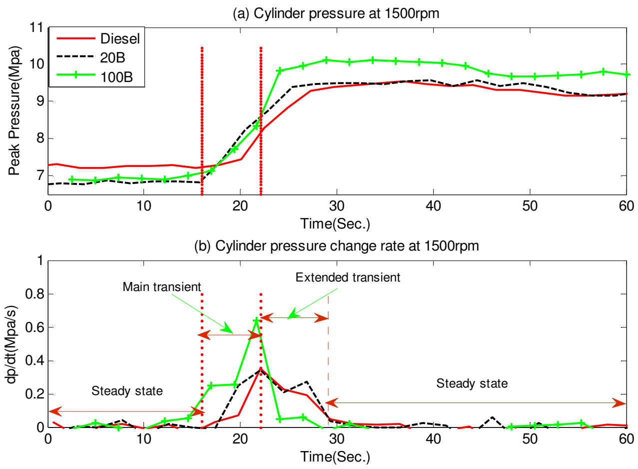

Fig.7(a) Variation of in-cylinder peak pressure with time during torque positive transient (b) rate of change in-cylinder peak pressure with time

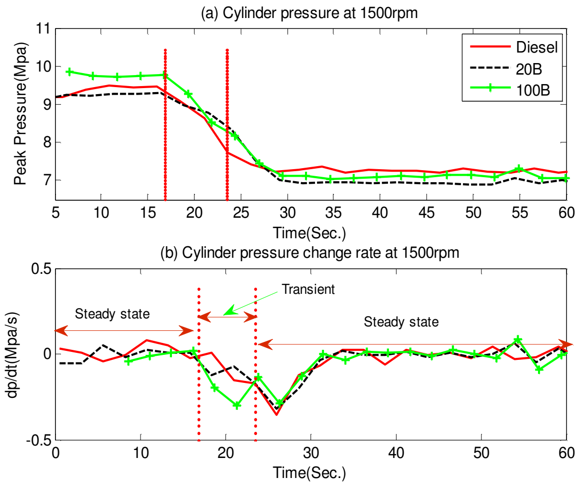

Fig. 8(a) Variation of in-cylinder peak pressure with time for during torque negative transient (b) rate of change in-cylinder peak pressure with time

3.2- Fuel Consumption Rate

The fuel flow rate has been measured by FMS-1000 gravimetric fuel measurement system during both steady and transient conditions. The variations of the fuel flow rate with the operating conditions have been reported here. Fig. 9 shows the variation of fuel flow rate of diesel and biodiesel blends during the speed transient of 1000 to 1500rpm and 1500 to 1000rpm at 420Nm load. It can be clearly seen that the fuel flow rate increases by 35% during the acceleration of the engine from 1000 to 1500 rpm and the fuel flow rate decreases by 33% during the deceleration of the engine from 1500 to 1000 rpm. The fuel flow rate increment with acceleration can be explained on the basis that when the engine speed increases the cylinder charging rate increases as a consequent fuel flow rate increases [19].

In addition, during acceleration the friction horsepower increases because of a drop in the mechanical efficiency to maintain a fixed torque output, leading to an increase in the fuel consumption rate [19]. Fig. 9(c-d) depicts that the fuel consumption of the engine running with 100B is higher than that of diesel by 16% during the acceleration and 14% during the deceleration transient operations respectively. This has occurred due to the effect of lower heating value of the biodiesel which is lower than the diesel by 11%. Previous researchers have also reported similar trends [20–23] in fuel consumption based on discrete engine speed tests.

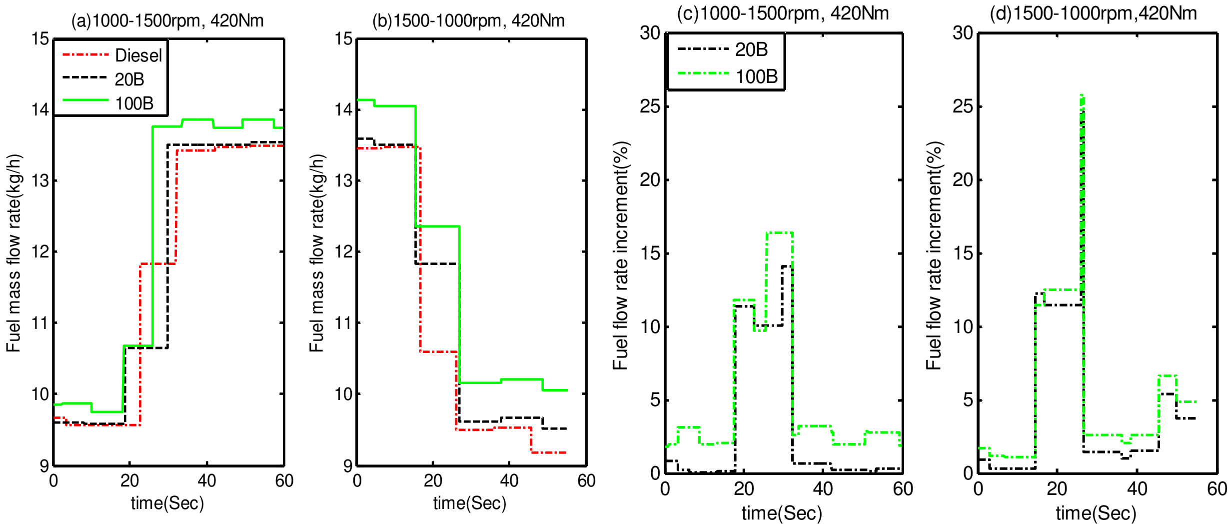

Fig. 9 Fuel flow rate profiles at 420Nm; (a) acceleration; (b) deceleration; (c) relative changes for acceleration; and (c) relative changes for deceleration

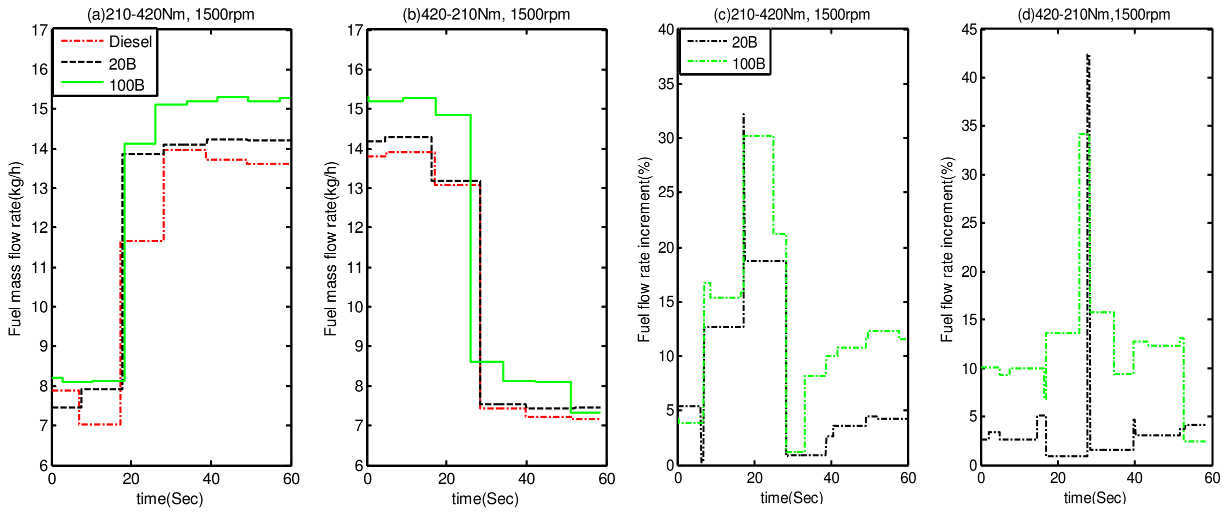

Fig. 10 Fuel flow rate profiles for torque change at 1500rpm; (a) acceleration; (b) deceleration; (c) relative changes for acceleration; and (c) relative changes for deceleration

The effects of the torque transient operation on fuel consumption rate for the engine running with diesel and two blends 20B and 100B are presented in Fig. 10. The fuel consumption rate increases by 31% during the positive torque transition of 210-420Nm at 1500rpm. Similarly, the fuel consumption rate decreases by 34% during the negative torque conditions of 420-210Nm. This is due to the increase in the fuel injection to attain the required higher total energy output at a given engine speed. Comparing the fuel consumption rates of CI engine running with the biodiesel blends and diesel, it can be seen in Fig. 10(c-d) that the engine running with the former resulted in higher fuel consumption rate by 17% and 15% for both positive and negative torque operations respectively.

3.2- Exhaust Gas Temperature

The exhaust gas temperature values obtained from the test engine running with diesel, 20B and 100B during speed transient of 1000-1500rpm and 1500-1000rpm and at a load of 420Nm are depicted in Fig. 11. It can be seen that the exhaust gas temperatures of the diesel and biodiesel blends do not show any significant difference for both acceleration and deceleration transient conditions. In both the conditions, the maximum difference between the exhaust gas temperature of the engine running with diesel and biodiesel blends is limited to 2%. The exhaust temperature increases from 600K to 710K during the acceleration operation and decreases from 710K to 630K during the deceleration transient operations. The reason behind this can be explained as when the engine accelerate from 1000rpm to 1500rpm, the amount of fuel injected to the cylinder also increases in order to maintain a constant engine torque output. As a result, the heat release rate and the exhaust gas temperature increases from burning of the fuels [19]. During the deceleration from 1500-1000rpm, the reverse phenomenon occurs in the cylinder.

The effects of the torque transition operation on exhaust gas temperature for the engine running with diesel, 20B and 100B are presented in Fig. 12. The exhaust temperature increases from 570K to 670K during the positive torque transient of 210-420Nm at a speed of 1500rpm (see Fig. 12(a)). Similarly, the exhaust gas temperature decreases during negative torque conditions of 420-210Nm. This is due to the increase in the fuel injection to attain the required higher total energy input.

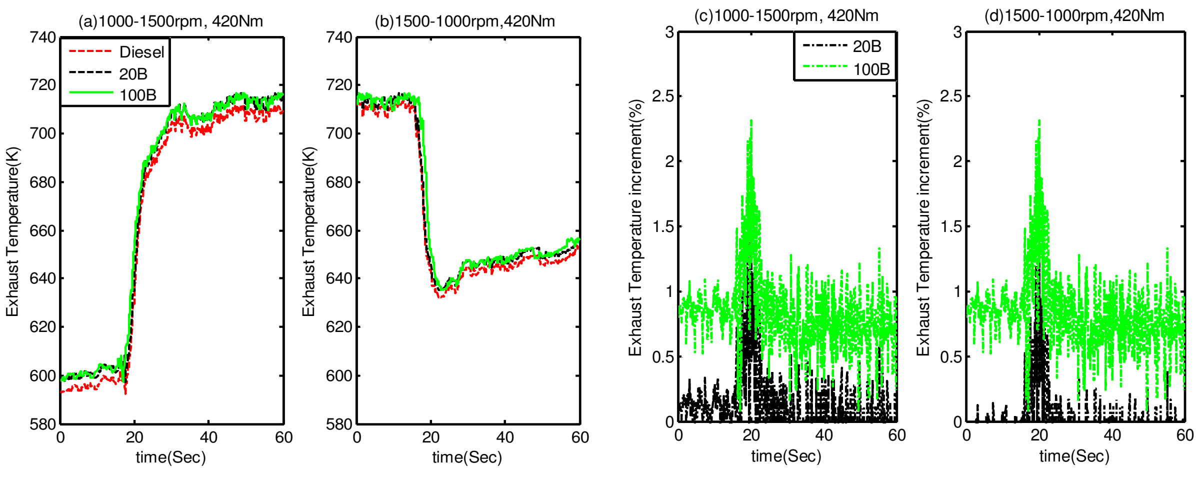

Fig. 11(a-b) Variation of exhaust temperature with time for CI engine running with biodiesel during speed transient at 420Nm (c-d) Variation of exhaust temperature percentage increment with time by using biodiesel blends during speed transient at 420Nm

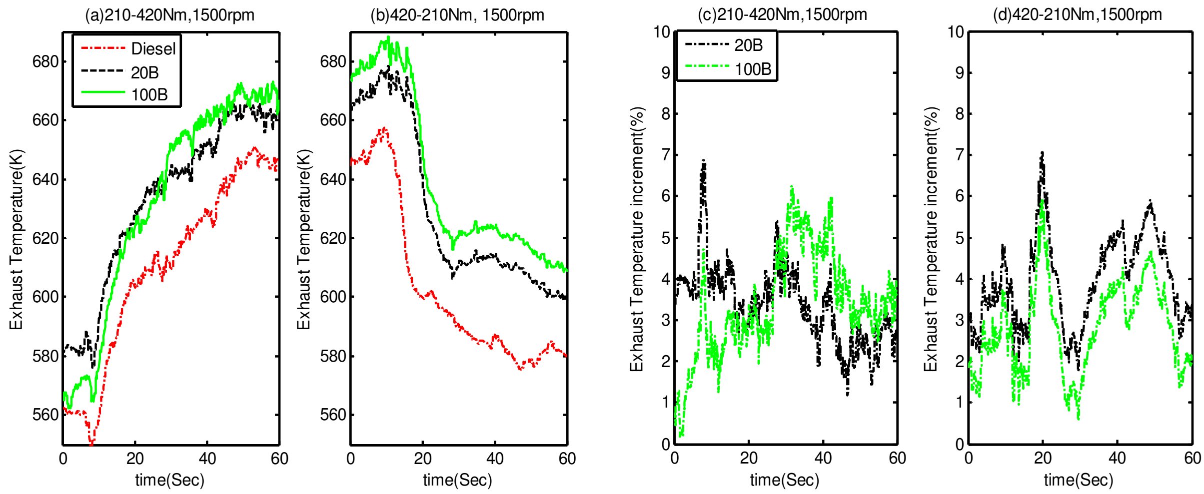

Fig. 12 (a-b) Variation of exhaust temperature with time for CI running with biodiesel during torque transition at 420Nm (c-d) Variation of exhaust temperature percentage increment with time by using biodiesel blends during torque transition at 420Nm

Comparing the exhaust temperature of engine running with the biodiesel blends and diesel, it can be seen in (Fig. 12(c-d)) that the engine running with the former resulted in higher exhaust gas temperature by 7% for both positive and negative torque operations. In addition, the exhaust temperature increases with increasing the biodiesel fraction in the blends. This can be explained on the basis that as biodiesel have 11% oxygen in its molecular structure, the oxygen molecule enhances the complete combustion of fuel in the cylinder. As a result the in-cylinder temperature increases and consequently the exhaust temperature increases[2],[3] .

The following summary can be drawn from the results obtained from both performance and emission studies during transient operation.

- The analysis conducted on the fuel flow rate shows that the fuel consumption of the engine running with 100B is higher than that of diesel by 16% and 14% for the acceleration and deceleration transient operations respectively. These values increased to 17% and 15% for positive and negative torque transition operations.
- In acceleration and deceleration conditions, the maximum difference between the exhaust temperature of engine running with diesel and biodiesel blends is less than 2%. During torque transition operations, the engine running with biodiesel has higher exhaust gas temperature than that of running with diesel by 7%.
- The peak cylinder pressure of the engine running with biodiesel blends is slightly higher than the engine running with diesel. The main reason for a higher in-cylinder pressure in the CI engine running with biodiesel could be due to the advanced combustion process being initiated by the easy flow-ability of biodiesel and its other relevant physical properties such as viscosity, density and bulk modulus.

References

[1] B. Tesfa, “Investigations into the Performance and Emission Characteristics of a Biodiesel Fuelled CI Engine under Steady and Transient Operating Conditions,” University of Huddersfield, 2011.

[2] J. Xue, T. E. Grift, and A. C. Hansen, “Effect of biodiesel on engine performances and emissions,” *Renewable and Sustainable Energy Reviews*, vol. 15, no. 2, pp. 1098–1116, Feb. 2011.

[3] M. Lapuerta, O. Armas, and J. Rodríguez-Fernández, “Effect of biodiesel fuels on diesel engine emissions,” *Progress in Energy and Combustion Science*, vol. 34, no. 2, pp. 198–223, Apr. 2008.

[4] O. Armas, J. J. Hernández, and M. D. Cárdenas, “Reduction of diesel smoke opacity from vegetable oil methyl esters during transient operation,” *Fuel*, vol. 85, no. 17–18, pp. 2427–2438, Dec. 2006.

[5] S. Samuel, D. Morrey, D. H. C. Taylor, and M. Fowkes, “Parametric Study into the Effects of Factors Affecting Real-World Vehicle Exhaust Emission Levels,” SAE International, Warrendale, PA, 2007-01-1084, Apr. 2007.

[6] M. F. J. Brunt, H. Rai, and A. L. Emtage, “The Calculation of Heat Release Energy from Engine Cylinder Pressure Data,” SAE International, Warrendale, PA, 981052, Feb. 1998.

[7] F. Payri, J. M. Luján, J. Martín, and A. Abbad, “Digital signal processing of in-cylinder pressure for combustion diagnosis of internal combustion engines,” *Mechanical Systems and Signal Processing*, vol. 24, no. 6, pp. 1767–1784, Aug. 2010.

[8] J. M. Desantes, J. Galindo, C. Guardiola, and V. Dolz, “Air mass flow estimation in turbocharged diesel engines from in-cylinder pressure measurement,” *Experimental Thermal and Fluid Science*, vol. 34, no. 1, pp. 37–47, Jan. 2010.

[9] M. Abu-Qudais, “Exhaust gas temperature for knock detection and control in spark ignition engine,” *Energy Conversion and Management*, vol. 37, no. 9, pp. 1383–1392, Sep. 1996.

[10] F. Morey and P. Seers, “Comparison of cycle-by-cycle variation of measured exhaust-gas temperature and in-cylinder pressure measurements,” *Applied Thermal Engineering*, vol. 30, no. 5, pp. 487–491, Apr. 2010.

[11] S. M. Aithal, “Modeling of NOx formation in diesel engines using finite-rate chemical kinetics,” *Applied Energy*, vol. 87, no. 7, pp. 2256–2265, 2010.

[12] A. Ibrahim and S. Bari, “A comparison between EGR and lean-burn strategies employed in a natural gas SI engine using a two-zone combustion model,” *Energy Conversion and Management*, vol. 50, no. 12, pp. 3129–3139, Dec. 2009.

[13] D. T. Hountalas, G. C. Mavropoulos, T. C. Zannis, and S. D. Mamalis, “Use of Water Emulsion and Intake Water Injection as NOx Reduction Techniques for Heavy Duty Diesel Engines,” SAE International, Warrendale, PA, 2006-01-1414, Apr. 2006.

[14] T. T. AL-Shemmeri and S. Oberweis, “Correlation of the NOx emission and exhaust gas temperature for biodiesel,” *Applied Thermal Engineering*, vol. 31, no. 10, pp. 1682–1688, Jul. 2011.

[15] B. Tesfa, R. Mishra, F. Gu, and A. D. Ball, “Water injection effects on the performance and emission characteristics of a CI engine operating with biodiesel,” *Renewable Energy*, vol. 37, no. 1, pp. 333–344, Jan. 2012.

[16] B. Tesfa, R. Mishra, F. Gu, and O. Gilkes, “Emission Behavior of a CI Engine Running by Biodiesel under Transient Conditions,” SAE International, Warrendale, PA, 2010-01-1280, Apr. 2010.

[17] A. J. Martyr and M. A. Plint, *Engine Testing: Theory and Practice*, 3rd Revised ed. Butterworth-Heinemann Ltd, 2007.

[18] B. Tesfa, R. Mishra, F. Gu, and N. Powles, “Prediction models for density and viscosity of biodiesel and their effects on fuel supply system in CI engines,” *Renewable Energy*, vol. 35, no. 12, pp. 2752–2760, Dec. 2010.

[19] C.-Y. Lin and H.-A. Lin, “Diesel engine performance and emission characteristics of biodiesel produced by the peroxidation process,” *Fuel*, vol. 85, no. 3, pp. 298–305, Feb. 2006.

[20] D. H. Qi, L. M. Geng, H. Chen, Y. Z. Bian, J. Liu, and X. C. Ren, “Combustion and performance evaluation of a diesel engine fueled with biodiesel produced from soybean crude oil,” *Renewable Energy*, vol. 34, no. 12, pp. 2706–2713, Dec. 2009.

[21] A. S. Ramadhas, C. Muraleedharan, and S. Jayaraj, “Performance and emission evaluation of a diesel engine fueled with methyl esters of rubber seed oil,” *Renewable Energy*, vol. 30, no. 12, pp. 1789–1800, Oct. 2005.

[22] O. Armas, K. Yehliu, and A. L. Boehman, “Effect of alternative fuels on exhaust emissions during diesel engine operation with matched combustion phasing,” *Fuel*, vol. 89, no. 2, pp. 438–456, Feb. 2010.

[23] C. Carraretto, A. Macor, A. Mirandola, A. Stoppato, and S. Tonon, “Biodiesel as alternative fuel: Experimental analysis and energetic evaluations,” *Energy*, vol. 29, no. 12–15, pp. 2195–2211, Oct. 2004.